Proceedings of the ASME 2010 International Mechanical Engineering Congress & Exposition
IMECE2010
November 12-18, 2010, Vancouver, British Columbia, Canada

IMECE2010-40571

HYBRID LIQUID-AIR TRANSPIRED SOLAR COLLECTOR: MODEL DEVELOPMENT AND SENSITIVITY ANALYSIS

Abdul Qadir
Graduate Student, Masdar Institute of Science and Technology
Abu Dhabi, United Arab Emirates

Peter R. Armstrong
Associate Professor, Masdar Institute of Science and Technology
Abu Dhabi, United Arab Emirates

ABSTRACT

The paper develops an analytical model of a novel hybrid liquid-air transpired solar collector which could simultaneously heat air and water for applications such as regeneration of liquid desiccants. An energy balance is performed, leading to a system of ODEs which is solved to obtain the air and water outlet temperatures of the collector. Three sets of sensitivity analyses have been performed on the collector varying the total thermal capacitance rates of the air and water$(\dot{m}c_p)_{total}$, ratio of air to total thermal capacitance rate$(\dot{m}c_{p\ ratio})$, and the usual boundary conditions of water inlet temperature T_{wi}, ambient temperature T_{amb}, solar radiation G and wind speed V_w. General performance curves for the collector with increasing $(T_{wi}-T_{amb})/G$ have been developed as a result of these analyses. It has been observed that a $\dot{m}c_{p\ ratio}$ between 0.3 and 0.4 provides with an optimal collector performance. Moreover at low $\dot{m}c_{p\ ratio}$s, the collector performance has been observed to be very sensitive to wind speed.

INTRODUCTION

The government of Abu Dhabi has ambitious plans of moving towards a sustainable society which includes the integration of solar energy to the energy mix of the emirate [1]. Over 60% of peak electricity usage in Abu Dhabi city is accounted due to cooling[2]. This, coupled with the high solar resource[3] during the summer, encourages the use of solar energy towards cooling applications. Moreover, the populous UAE coastal region has a very humid climate, thus solar regenerated desiccant latent cooling may be attractive.

Previously there have been studies towards the use of flat plate collectors and transpired solar collectors in desiccant regeneration applications[4]. However the use of both glazed and unglazed flat plate collectors as well as transpired collectors has proved economically unfeasible [5]. The transpired and unglazed collectors exhibit low efficiencies when heating air and water to a regeneration temperature of 70C while glazed flat plate collectors have higher efficiencies but are significantly more expensive.

Thus this paper formulates a simple steady state model of a potentially economical unglazed, hybrid, transpired liquid-air collector (UHTLAC) that simultaneously heats water and ambient air. We postulate that this type of collector could be especially useful for desiccant regeneration in desiccant cooling cycles because the regeneration process needs a continuous supply of fresh air to carry away vapor released when the weak LiBr solution is heated moderately to a temperature below its bubble point.INSERT A SCHEMATIC HERE showing collector, regenerator and dehumidifier (Thus the heat gain of the UHTLAC suction air, whose main purpose in this application is to suppress convection loss, can be put to good use in the desiccant regeneration process.

Using the steady-state model we are able to explore the sensitivity of UHTLAC collection efficiency to variations in air and water flow rate, water inlet temperature, and ambient conditions of temperature, incident solar irradiation, and wind speed.

NOMENCLATURE

A	Collector area (m^2)
$q_{rad,loss}$	Radiation loss per unit length (W/m)
$q_{conv,loss}$	Convection loss per unit length(W/m)
T_m	Mean plate temperature (K)
T_{amb}	Ambient temperature (K)
T_{pl}	Plate temperature (K)
Ta	Air temperature (K)
Tw	Water Temperature (K)
Tsky	Sky Temperature (K)
$\dot{m}_a$	Mass flow rate of air (kg/s)
$\dot{m}_w$	Mass flow rate of water (kg/s)
$(\dot{m}c_p)_{total}$	Total thermal capacitance of air and water
$\dot{m}c_{p\ ratio}$	Ratio of ${\dot{m}c_p}_{air}$ to ${\dot{m}c_p}_{total}$
c_{pa}	Specific heat of air (kJ/kgK)
c_{pw}	Specific heat of water (kJ/kgK)
W	Width of collector (m)
L	Length of collector (m)
U_l	Total top loss coefficient (W/m^2K)
U_a	Heat transfer coefficient for air behind collector (W/m^2K)
G	Incident solar radiation (W/m^2)
P	Perimeter of plenum cross section (m)

Greek letters:

ϵ	Emissivity of collector plate
σ	Stephan-Boltzmann constant

Subscripts:

i	inlet
o	outlet

METHODOLOGY

The collector configuration? is that of a fin tube flat plate collector in which the plate used is perforated in the manner of a conventional transpired solar collector[6]. Thus water is heated in tubes that run from the base of the collector to the top where it exits via a standard header tube, while the air is sucked through the plate and heated as it travels behind the plate from a given point of entry to the top where it exits via an air duct. A sketch of the collector is shown in figure 1.

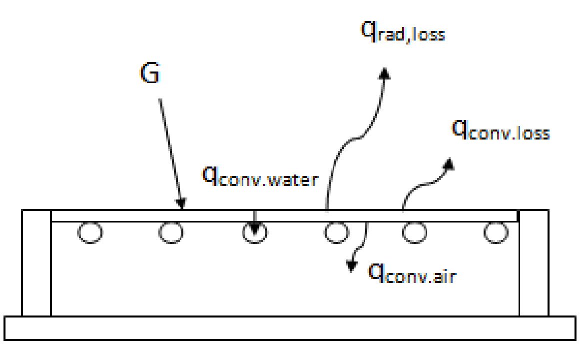

Figure 1: Sketch of end view of collector; air and water flows below the plate are into the page in the y direction

The energy balance on a differential element of the collector with unit width is shown in figure 2.

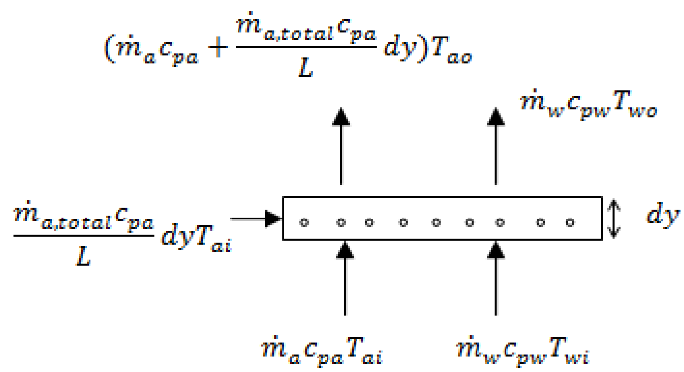

Figure 2: Differential element of the collector in plan view

The energy balances for water and air respectively are:

$$\dot{m}_w c_{pw} \frac{dT_w}{dy} = WG - WU_l(T_{pl} - T_{amb}) - WU_a(T_{pl} - T_a) - W\frac{\dot{m}_a c_{pa}}{A}(T_a - T_{amb}) \quad (1)$$

$$\frac{d\dot{m}_a}{dy} c_{pa} \frac{dT_a}{dy} = WU_a(T_{pl} - T_a) \quad (2)$$

The mass balance for the air entering each element of the collector was:

$$\frac{d\dot{m}_a}{dy} = \frac{\dot{m}_{a,total}}{L} \quad (3)$$

In the above expressions, U_l is a total heat loss coefficient from the front of the plate that is modified[7] to account for radiation to the sky whose effective temperature may differ from that of ambient air. Thus U_l involves both convective and radiative losses per unit plate area given by:

$$q_{rad,loss} = \epsilon\sigma 4{T_m}^3(T_{pl} - T_{sky}) \quad (4)$$

$$q_{conv,loss} = U_{wind}(T_{pl} - T_{amb})) \quad (5)$$

Where

$$Tm = (Tpl + Tsky)/2 \quad (6)$$

and

$$U_{wind} = 0.82 \frac{V_w \mu_a \rho_a c_{pa}}{V_s L} \quad (7)$$

where

$$V_s = \frac{\dot{m}_a}{\rho_a A} \quad (8)$$

U_{wind} is the convective heat transfer coefficient for laminar forced convection over a flat plate with suction found in literature[6]. Thus U_l can be expressed as the sum of convective and radiative heat losses with respect to (T_{pl}-T_{amb}).

$$U_l = U_{wind} + \frac{q_{rad,loss}}{(T_{pl} - T_{amb})} \quad (9)$$

In equations (1) and (2) the U_a term is the heat transfer coefficient for the air heated at the back of the plate. To derive this term, the air flow at the back of the collector is assumed laminar and flowing through a rectangular duct with the front plate heated while the back plate is insulated. Moreover the width of the collector is considerably larger than the plenum depth and thus the ratio of the width to depth is approximated as infinity. Therefore the Nusselt number is 4.86[8] and U_a is calculated as:

$$U_a = \frac{Nu_D k_{air}}{D_H} \tag{10}$$

where

$$D_H = \frac{4A}{P} \tag{11}$$

In order to simplify the otherwise complex nature of the equations, the plate temperature of each finite element was approximated as the outlet water temperature of the previous element. Moreover, the outlet temperature of the air sucked through the plate was approximated as the outlet air temperature of the air moving through the plenum of the previous element. The two energy balance equations and the mass balance equation were then solved simultaneously using the forth/fifth order Runge-Kutta method in the computation software Matlab™[9].

Thus by solving these equations, the outlet air and water temperature through the collector and consequently the efficiency of the collector were obtained.

RESULTS

Sensitivity analysis of the collector model was carried out to observe the performance of the collector by varying the ambient temperature(T_{amb}), inlet water temperature(T_{wi}), collector emissivity(ϵ) and total thermal capacitance of air and water($(\dot{m}c_p)_{total}$=$\dot{m}_w c_{pw} + \dot{m}_a c_{pa}$). Moreover for each analysis, the ratio of thermal capacitance of air to total thermal capacitance ($\dot{m}c_{p\ ratio}$) was varied to observe the effect it had on the efficiency of the collector along with the other varying parameter. Throughout the analysis, the collector dimensions, weather conditions and solar radiation have been taken as constant and their values are displayed in Table 1.

The first analysis was aimed at obtaining the performance of the collector with different $(\dot{m}c_p)_{total}$ entering the collector along with a range of values of $\dot{m}c_{p\ ratio}$ from 0.1 to 0.9. The range of values of $(\dot{m}c_p)_{total}$ was from 5W/m2K to 25W/m2K at five equal intervals and the ambient temperature was maintained at 305K. The results obtained for these analyses are shown in figure 3.

The second set of analysis was performed by varying the inlet temperature of the water from 305K to 345K to obtain the efficiency of the collector. The ambient temperature for this analysis was fixed at 305K and the $(\dot{m}c_p)_{total}$ was fixed at 15W/m2K. The emissivity and $\dot{m}c_{p\ ratio}$ was also varied to obtain a family of curves for emissivities and $\dot{m}c_{p\ ratio}$s of 0.1, 0.5 and 0.9. The results are shown in figures 5, 6 and 7.

Table1: Geometric parameters, fluid properties and baseline conditions used in the sensitivity analysis

Property	Value
Solar radiation (S)	800W/m^2
Wind speed(V_w)	3 m/s
Humidity	50%
Air temperature(Tamb)	305K
Air density(ρ_a)	1.184kg/m^3
Air Viscosity (μ_a)	1.849*10^{-5} Ns/m^2
Air Cp (c_{pa})	1.007kJ/kgK
Length of collector (L)	2m
Width of collector (W)	1m
Plenum depth (D)	0.1m
Perimeter of plenum cross section	2.2m

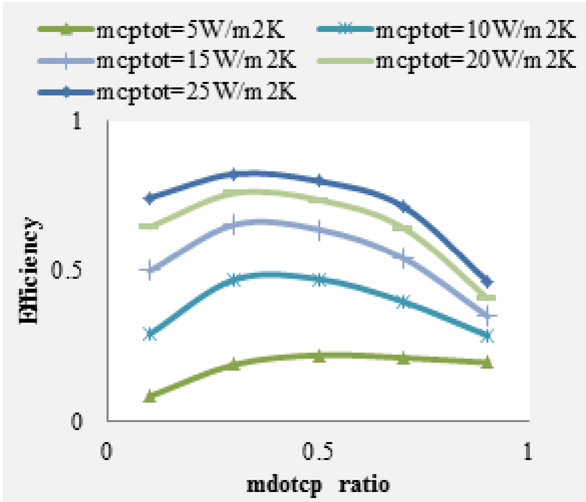

Figure 3: Efficiency vs. $\dot{m}c_p$ ratio for range of $(\dot{m}c_p)_{total}$ with $T_{w,i}$ = T_{amb} = 32°C

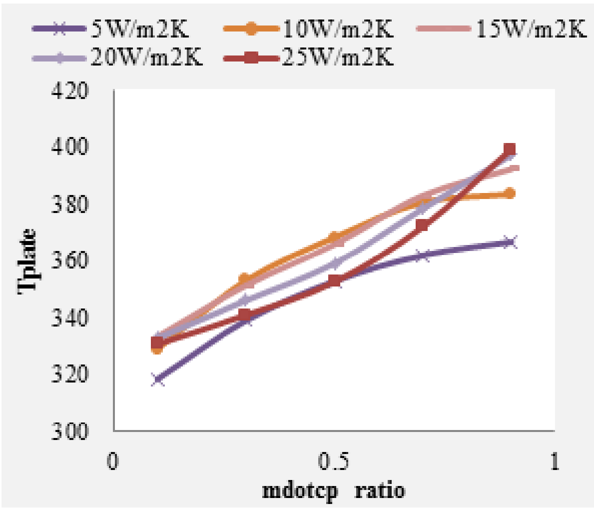

Figure 4: Plate temperature vs. $\dot{m}c_{p\ ratio}$ for range of $(\dot{m}c_p)_{total}$ with $T_{w,i}$ = T_{amb} = 32°C

The third analysis aims at developing standard performance curves for the collector for a wider range of varying parameters. For this analysis $(\dot{m}c_p)_{total}$ has been kept constant at 15W/m^{2}K , while $\dot{m}c_{p\ ratio}$, V_w, T_{wi}, T_{amb} and G have been varied. The ranges of values for which these parameters have been varied are displayed in Table 2. The results from this analysis are illustrated in Figures 8&9.

Table 2: Conditions used in sensitivity analyses

Parameter	Values
(1)Air temperature(T_{amb})	295,305,315(K)
(1)Water inlet temperature(T_{wi})	305,325,345 (K)
(1)Air to total thermal capacity ratio($\dot{m}c_{p\ ratio}$)	0.1, 0.3, 0.5, 0.7, 0.9
(2)Solar radiation (G)	300, 600, 900 (W/m^2)
(2)Wind speed(V_w)	0, 2, 5 (m/s)

(1) G and V_w are fixed for the first two sensitivity exercises at values given in Table 1.
(2) G and Vw are only varied for the standard collector performance curve plots (figures 8 &9) that show wind speed sensitivity.

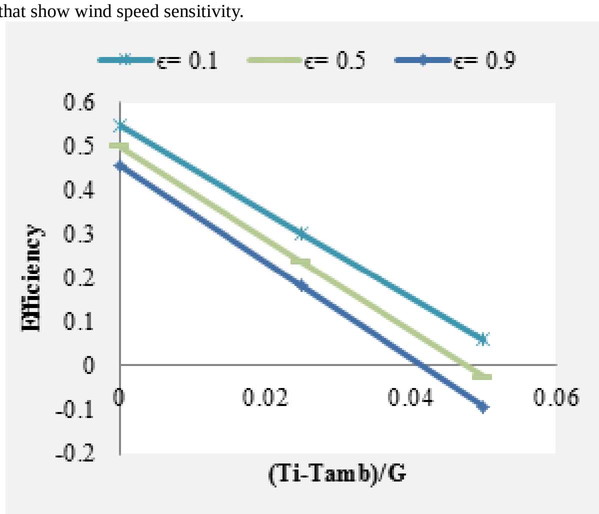

Figure 5: Efficiency vs. ΔT/G for $\dot{m}c_{p\ ratio}$= 0.1 and T_{amb} = 32°C

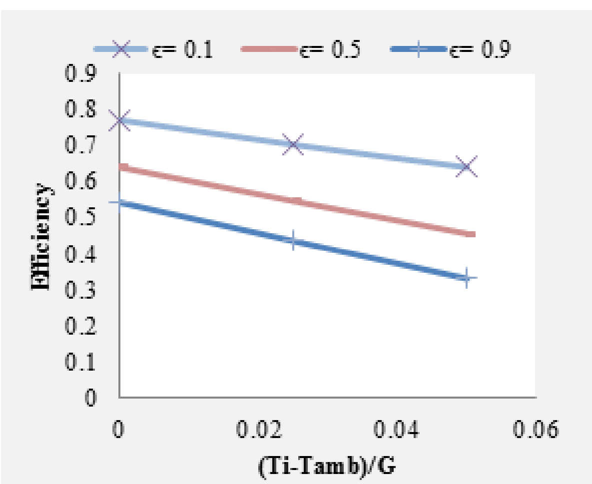

Figure 6: Efficiency vs. ΔT/G for $\dot{m}c_{p\ ratio}$= 0.5 and T_{amb} = 32°C

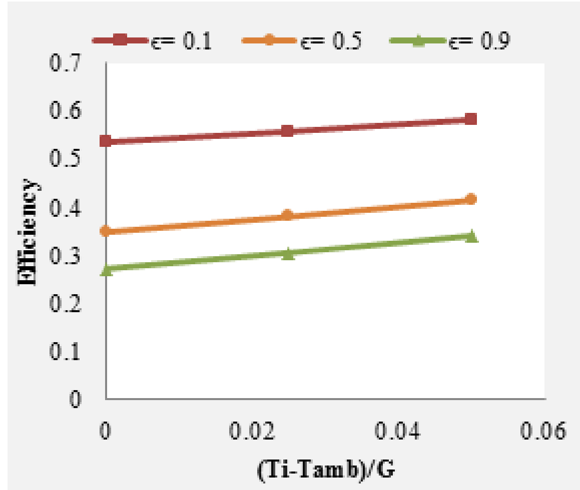

Figure 7: Efficiency vs. ΔT/G for $\dot{m}c_{p\ ratio}$= 0.9 and T_{amb} = 32°C

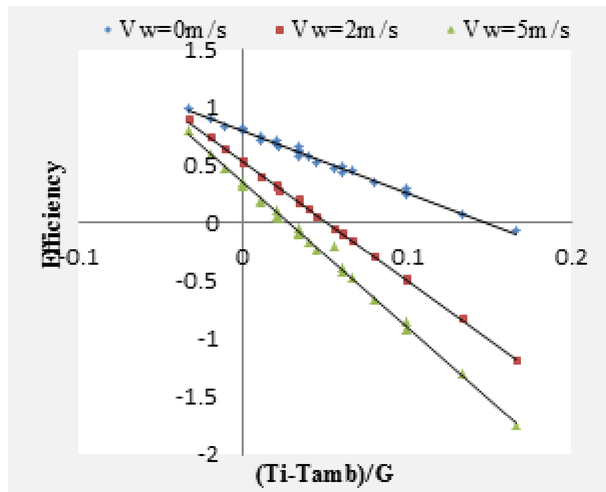

Figure 8: Efficiency vs. ΔT/G for $\dot{m}c_{p\ ratio}$= 0.1, $(\dot{m}c_p)_{total}$=15W/m^{2}K and varying G, T_{amb}, T_{win}, and V_w.

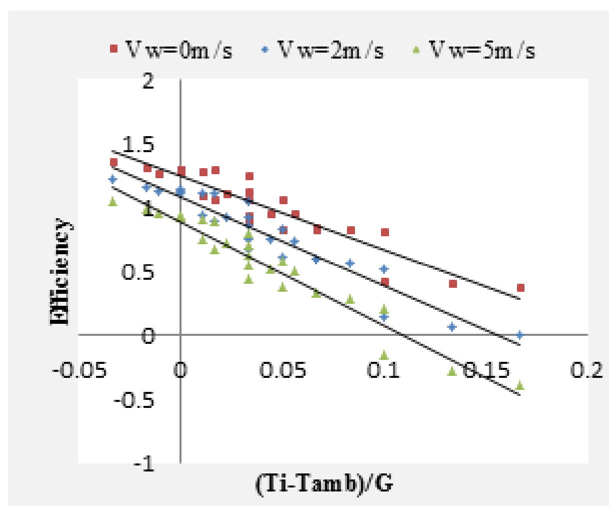

Figure 9: Efficiency vs. ΔT/G for $\dot{m}c_{p\ ratio}$= 0.5, $(\dot{m}c_p)_{total}$=15W/m^{2}K and varying G, T_{amb}, T_{win}, and V_w.

DISCUSSION

The results from the first analysis show that the efficiency of the collector is highest when $\dot{m}c_{p\ ratio}$ is between 0.3 and 0.4 for $(\dot{m}c_p)_{total}$ greater than 5W/m2K. It also shows the general trend of increasing efficiency with increasing $(\dot{m}c_p)_{total}$. The existence of a maximum efficiency point at an intermediate ratio of air-to-total flow rate may be attributed to the fact that as the $\dot{m}c_{p\ ratio}$ increases, the convective losses due to wind decrease, leading to an increase in the efficiency of the collector. However after a certain increase in $\dot{m}c_{p\ ratio}$, further increase in the ratio has very little effect on the convective losses. Thus as the mass flow rate of water decreases, the plate temperature increases steadily leading to a rapid increase in the radiative losses and, consequently, a noticeable decrease in collector efficiency.

The second analysis shows the trend of decreasing efficiency of the collector for a $\dot{m}c_{p\ ratio}$ of 0.1 and 0.5 as $(T_i\text{-}T_{amb})/G$ is increased (Figures 5&6). On the other hand, the efficiency of the collector increases for a high $\dot{m}c_{p\ ratio}$ of 0.9. This shows that the collector exhibits the characteristic of an unglazed flat plate collector for the low $\dot{m}c_{p\ ratio}$. However the increasing efficiency of the collector for a high $\dot{m}c_{p\ ratio}$ can be explained by the higher heat transfer rate from the water to the air due to a larger temperature gradient, keeping in mind that the inlet air is at ambient temperature.

The results from the third analysis show that there is a general trend of decrease in the efficiency of the collector as ΔT/G is increased. The trend is highlighted by adding a line of best fit to the results obtained from the analysis. Furthermore it may be seen that when $\dot{m}c_{p\ ratio}$ is low (Figure 8), the efficiency of the collector is very sensitive to the wind speed. This phenomenon may be explained by the fact that at a low $\dot{m}c_{p\ ratio}$, the convective losses from the collector are weakly suppressed and thus an increase in the wind speed greatly increase the convective losses, hence decreasing the collector efficiency considerably.

FUTURE WORK

The next step in the study of the UHTLAC is refinement and experimental validation of the model. In this regard, a test rig based on a $2m^2$ collector is being built at MIST.

If the air flow ratio can be adjusted with relatively small adverse impact on the regeneration process, there is clearly an opportunity to maintain high overall efficiencies over a range of conditions by proper balancing of the air and water flow rates. A valid model of the regeneration process is needed before the control problem can be properly addressed.

In addition to the flow balance control problem, the opportunity to improve system performance by adjusting the distribution of collector plate porosity, currently modeled such that uniform face velocity is achieved, may be explored.

Finally, it would be useful to find a semi-empirical model of the collector thermal performance to avoid having to solve the detailed collector equations at every time step of a system simulation.

CONCLUSION

Afinite difference collector model of a novel hybrid liquid air collector has been developed and the outlet water and air temperatures from the collector computed through solving a system of ODEs. Key parameters of the model have been varied to assess the impact on the performance of the collector.

Increasing the $(\dot{m}c_p)_{total}$ has shown an increase in the efficiency of the collector for all values of $\dot{m}c_{p\ ratio}$. Moreover, an increase of the $\dot{m}c_{p\ ratio}$ from 0.1 to about 0.4 at a constant $(\dot{m}c_p)_{total}$ has shown an increase in the efficiency of the collector while further increase in $\dot{m}c_{p\ ratio}$ has led to a decrease in the efficiency. Furthermore, an increase of $(T_i\text{-}T_{amb})/G$ has shown a decrease in the efficiency of the collector for $\dot{m}c_{p\ ratio}$s of 0.1 and 0.5 while for a $\dot{m}c_{p\ ratio}$ of 0.9, the efficiency has increased. Lastly, for a low $\dot{m}c_{p\ ratio}$ of 0.1, the efficiency of the collector shows considerable sensitivity to an increase in wind speed, showing that the convective losses are only marginally suppressed at this $\dot{m}c_{p\ ratio}$.

In order to obtain more accurate results from the simulations, the heat transfer coefficient for the air at the front face of the collector and holes need to be examined.

REFERENCES

1. Reiche, D., *Renewable Energy Policies in the Gulf countries: A case study of the carbon-neutral Masdar City in Abu Dhabi.* Energy Policy, 2010. **38**: p. 378-382
2. Mokhtar, M., et al., *Systematic comprehensive techno-economic assessment of solar cooling*

   technologies using location-specific climate data. Applied Energy, 2010.
3. Islam, M.D., et al., *Measurement of solar-energy (direct beam radiation) in Abu Dhabi, UAE.* Renewable Energy, 2010. **35**: p. 515-519.
4. H.M Henning, T.E., C. Hindenburg, I.S. Santamaria, *The potential for solar energy use in desiccant cooling cycles* International Journal of Refrigeration, 2001. **24**: p. 220-229.
5. Pesaran, A.A. and K. Wipke, *DESICCANT COOLING USING UNGLAZED TRANSPIRED SOLAR COLLECTORS*, in *Solar '92*, S.M. Burley and M.E. Arden, Editors. 1992, American Solar Energy Society: Cocoa Beach Flordia.
6. Kutscher, C.F., C.B. Christensen, and G.M. Barker, *Unglazed Transpired Solar Collectors: Heat Loss Theory.* Journal of Solar Energy Engineering, 1993. **115**(3): p. 182-188.
7. Duffie, J. and W. Beckman, *Solar Engineering of Thermal Processes*. 1980: John Wiley & Sons Inc.
8. Incropera, et al., *Fundamentals of Heat and Mass Transfer*. 2006: Wiley.
9. *MATLAB*. 2008, The MathWorks, Inc.